Iran Polym J (2015) 24:715–724
DOI 10.1007/s13726-015-0357-9

ORIGINAL PAPER

Melt rheology of linear and long-chain branched polypropylene blends

Mahshid Maroufkhani[1] · **Nadereh Golshan Ebrahimi**[1]

Received: 22 July 2014 / Accepted: 28 June 2015 / Published online: 21 July 2015

Abstract The miscibility of linear polypropylene (L-PP) and long-chain branched polypropylene (LCB-PP) blends was studied in relation to the rheological behavior in shearing and elongational deformations of the blends. The rheological properties of four commercial L-PPs with different molecular weights were studied by adding 10, 25, 50, and 75 wt% of LCB-PP to L-PP. The linear viscoelastic properties such as complex viscosity and weighted relaxation spectrum were determined as functions of LCB-PP content. According to the obtained rheological data, the LCB-PP showed a higher zero-shear viscosity and a longer relaxation time than the L-PPs. The linear viscoelastic properties showed an increase in the molecular weight and branched content of the L-PP with a reduction in miscibility. Furthermore, good predictions of linear viscoelastic properties for miscible and immiscible blends were achieved by applying the Palierne model. In uniaxial elongational tests, the L-PP showed no strain hardening behavior. By contrast, the addition of 10 wt% LCB-PP to L-PP resulted in strain hardening behavior at all strain rates. Hence, the strain hardening behavior of the blends was enhanced with LCB-PP content. The elongational viscosity data of the L-PP and LCB-PP and their blends were studied by employing the Molecular Stress Function (MSF) model which could predict the strain hardening behavior of the blends.

Keywords Polypropylene · Long-chain branched · Rheology · Miscibility · Molecular Stress Function

List of symbols

G'	Elastic modulus
G''	Loss modulus
G^*	Complex modulus
η^+	Complex viscosity
ω	Frequency
LCB-PP	Long-chain branched polypropylene
L-PP	Linear polypropylene
η_0	Zero-shear viscosity
$H(\lambda)$	Continuous spectrum function
g_i	Relaxation modulus
λ_i	Relaxation time
MSF	Molecular Stress Function
ϕ_β	Weightfraction of branched component
α	Interfacial tension
R_v	Average radius of droplets
a	Diameter of tube segment
$\sigma(t)$	Extra stress tensor
f	Molecular Stress Function
$S_{\mathrm{DE}}^{\mathrm{IA}}$	Strain measure of the Doi-Edwards model
S_{DE}	Second-order orientation tensor
$\mathbf{u}'$	Unit vector
u'	Length of unit vector
η_{E}^+	Transient elongational viscosity

Introduction

Isotactic polypropylene is one of the leading and fast growing thermoplastic polymers in the world due to its desirable and beneficial properties such as low density, high melting point, high chemical resistance, and low cost. However, commercial polypropylene produced by Ziegler–Natta or metallocene catalysts has linear chains and a relatively narrow molecular weight distribution [1–3]. Linear

---

✉ Nadereh Golshan Ebrahimi
ebrahimn@modares.ac.ir

[1] Polymer Engineering Department, Chemical Engineering Faculty, Tarbiat Modares University, P.O. Box: 14115-114, Tehran, Iran

polypropylene has relatively low melt strength and exhibits no strain hardening, and as a result its application is restricted in processes where elongational properties, such as thermoforming, foaming, and blow molding are dominant [4, 5]. It is well known generally that the presence of branching improves the physical properties of polyolefins. Various investigations have shown that the phase behavior of polyethylene blends depends strongly on the presence of short or long branches. For the improvement of the melt properties of polypropylene, many attempts have been performed by some researchers [6–8]. Among these methods, introducing branches onto the backbone of commercial PP seems to be a more efficient approach because of its accessibility to industrialization and less cost [9]. Since the presence of LCB is generally known to enhance the melt strength of polymer, several approaches have been developed to synthesize long-chain branched polypropylene [10, 11]. Long-chain branches are commonly introduced to linear PP via electron beam or gamma irradiation [12, 13] and chemical modification [14, 15]. In the literature, the molecular structure and rheological properties of synthesized LCB-PPs has been investigated in details [16–18]. Compared to linear PP, LCB-PP shows a more pronounced shear-thinning behavior, a significant strain hardening and higher elasticity. The higher cost of LCB-PP leads researchers to use linear and long-chain branched polypropylene blends. In several cases, the foaming behavior of blends of linear and long-chain branched polypropylene were studied. Various studies have indicated that the foam morphologies of L-PP and LCB-PP blends are more uniform than those of neat L-PP. It was found that the strain hardening of branched polypropylenes caused high melt strength in addition to significant homogeneity of deformation in the elongational experiments [19, 20], which led to form foams with higher expansion ratios than L-PP [21].

In several cases the rheological behavior of blends of L-PP and LCB-PP has been investigated. It has been demonstrated that LCB-PP shows a more pronounced shear thinning; a higher elasticity and a significant strain hardening behavior compared to L-PP. Stange et al. [9] realized that the blending of L-PP with LCB-PP influences the rheological properties, especially the elongational behavior of L-PP. In addition, they found that the magnitude of strain hardening changed only slightly for the blends with higher than 25 wt% of LCB-PP, but a change of the dependency of the strain hardening on the strain rates occurred. McCallum et al. [22] concluded that the blending of L-PP and LCB-PP not only enhanced the melt strength, but the mechanical properties increased as well. Fang et al. [23] showed that increasing the length of short branches in metallocene LLDPEs with comparable molecular weights LDPE, could improve the miscibility of LLDPE/LDPE blends. Wagner et al. [24] investigated the elongational viscosities of blends of L-PP and LCB-PP and concluded that for the extruded LCB-PP a refining effect was observed. Tabatabaei et al. [25] found that the degree of crystallinity of the L-PP and LCB-PP blends first increased by adding small amounts of branched content but decreased by further addition.

Table 1 Main characteristics of neat polypropylene grades

Material	Trade name	MFR (g/10 min)	η_0^a (Pa s)	η_0^b (Pa s)	M_w (g/mol)
L-25	Z30S	25	2.45×10^3	2.73×10^3	2.33×10^5
L-9	HP510M	9	5.89×10^3	6.22×10^3	2.99×10^5
L-6	C30S	6	9.59×10^3	10.24×10^3	3.44×10^5
L-3.2	RG1104K	3.2	15.6×10^3	17.39×10^3	3.92×10^5
LCB-2.5	Pro-fax PF814	2.5	22.8×10^3	23.1×10^3	N/A

[a] Zero-shear viscosity values obtained from Maxwell model at $T = 180$ °C

[b] Zero-shear viscosity values obtained from the area under the weighted relaxation spectrum curves, $T = 180$ °C

This study aims to characterize the shear and elongational rheological properties of blends of L-PP and LCB-PP in detail as well as the applicability of "Molecular Stress Function" model for the blends. Our work focuses on the effect of molecular weight on the rheological properties of the blends. One of the novelties of this study is the verification of miscibility of polypropylene blends via rheological curves instead of other characterization methods due to its sensitivity to the molecular structure. The elongational viscosities of the blends were quantified with the MSF model.

Experimental

Materials

Four commercial linear polypropylenes (L-25, L-9, L-6, and L-3.2) were selected. The L-25 and L-6 were supplied by Iranian Shazand and Marun Petrochemical Companies with a melt flow rate (MFR) of 25 g/10 min (under ASTM conditions of 230 °C and 2.16 kg) and 6 g/10 min, respectively. The L-9 and L-3.2 were obtained from Iranian Jam Polypropylene Company and Regal Petrochemical Company with MFR of 9 g/10 min and 3.2 g/10 min, respectively. The commercial branched polypropylene (LCB-2.5) was produced by Basell. The molecular weights of the linear samples were obtained from the relation between the zero-shear viscosity and the molecular weight [26]. The main characteristics of testing materials are shown in Table 1. All PPs used in this work have a density about 0.9 g/cm^3.

A series of samples containing a range of LCB-PP contents (LCB-PP/L-PP weight ratios of 10/90, 25/75, 50/50, and 75/25) were prepared, as outlined below in the blend preparation section. All the pure samples were subjected to the same processing conditions in order to make sure that all of them have similar thermal history.

Blend preparation

Blends of L-PP and LCB-PP were prepared in a Brabender internal mixer at 210 °C and a rotor speed of 30 rpm for approximately 10 min (time to reach a constant torque). To avoid the thermal degradation of the polymers, 2000 ppm of an antioxidant (Irganox B225 from CibaGeigy) was used.

Rheological characterization

A hot press was used to form the compression molded disks that were 2 mm in thickness and 25 mm in diameter, at 200 °C. The dynamic melt rheological measurements were carried out using a controlled stress rheometer MCR-501 (by Anton Paar) in the oscillatory mode using parallel plate fixtures with 25 mm in diameter and a gap of 1.5 mm. All the measurements were carried out at 180 °C under a nitrogen atmosphere to limit degradation. Time sweeps confirmed that the samples did not degrade during the experiment. All the elongational viscosity measurements were performed using the SER HV-A01 model of the SERuniversal testing platform from Xpansion instrument. The rectangular samples with dimensions of 17 × 10 mm^2 and thickness of about 0.5 mm were used.

Strain sweeps were performed to ensure that the measurements were within the linear viscoelastic regime. The storage modulus (G'), loss modulus (G'') and complex viscosity (η^*) were measured as a function of the angular frequency (ω) at frequencies ranging from 0.02 to 600 rad/s.

Results and discussion

Rheological characterization of neat PPs

Figure 1 summarizes the complex viscosities of neat PPs as a function of angular frequency. The shear-thinning behavior of LCB-PP is more pronounced due to the presence of long-chain branches. In addition, with increasing the molecular weight of the L-PP the shear-thinning behavior is more pronounced and the transition zone from Newtonian plateau to the power-law flow region becomes smaller.

The plot of the loss angle, δ, as a function of frequency is plotted in Fig. 2. A uniform decrease in the loss angle is observed for the linear polypropylenes. At low frequencies the elasticity of the LCB-2.5 is larger compared to that of the L-PPs due to the presence of more

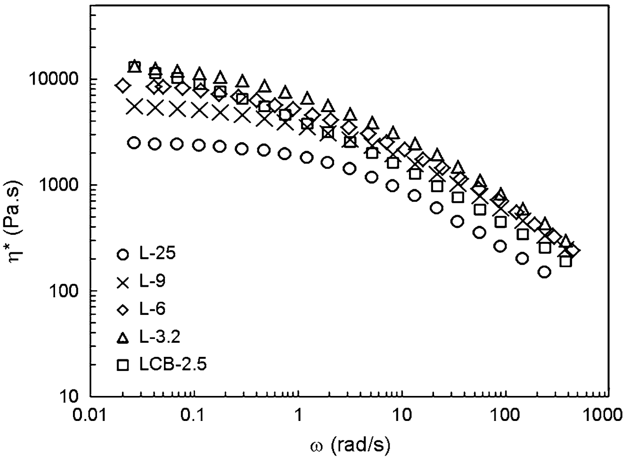

Fig. 1 Complex viscosity as a function of frequency for neat PPs at $T = 180$ °C

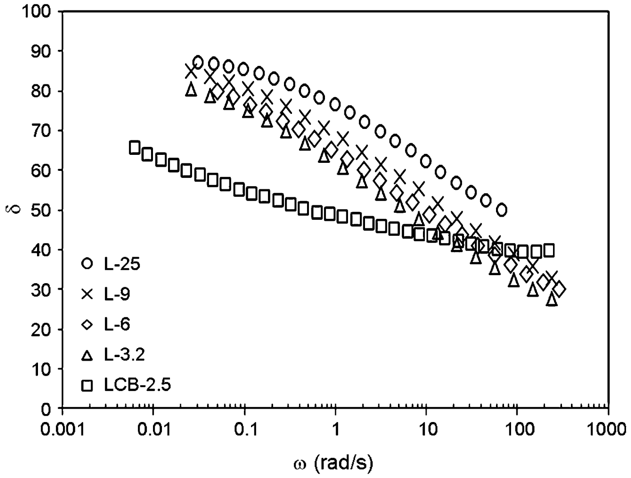

Fig. 2 Loss angle as a function of frequency for neat PPs at $T = 180$ °C

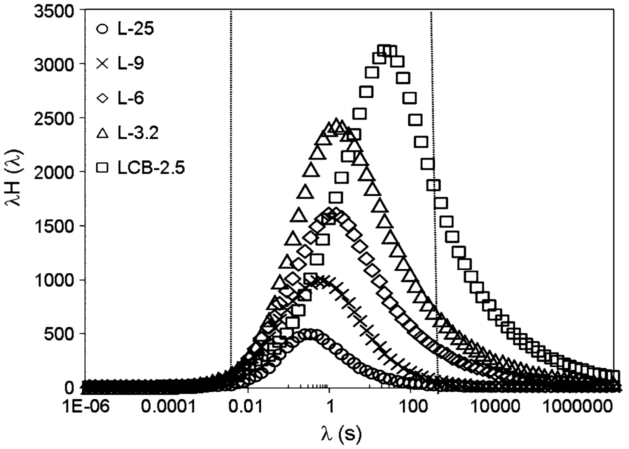

Fig. 3 Weighted relaxation spectra for neat PPs at $T = 180$ °C (*dash lines* represent the range of frequencies covered during experiments)

entanglements as a consequence of long-chain branches. As a result of more shear-thinning behavior, the number of entanglements in the LCB-2.5 (Fig. 1) decreases with increasing frequency. At high frequencies the LCB-2.5 shows a flexion in the curve with a trend to a plateau. It has been shown that the extent and the breath of the plateau is related to the weight fraction of the branched chains [27].

The weighted relaxation spectra of the neat polypropylenes obtained using the NLREG (non-linear regularization) software [28] are shown in Fig. 3 to compare the relaxation behavior of the L-PPs and LCB-2.5 (the limit of frequencies within the experiment is shown as dashed lines). The area under the relaxation spectrum indicates the zero-shear viscosity of the melt which is reported in Table 1. To verify the accuracy of the spectra, the zero-shear viscosities of the samples obtained from the area under the relaxation spectra:

$$\eta_0 = \int_{-\infty}^{+\infty} \lambda H(\lambda) \mathrm{d}(\ln \lambda) \tag{1}$$

were compared with the Maxwell model

$$\eta_0 = \sum g_i \lambda_i, \tag{2}$$

where g_i and λ_i are the relaxation modulus and relaxation time, respectively. A good agreement between these data is observed (Table 1). As seen in Fig. 3, with increasing the molecular weight in the L-PPs the position of the peaks shifts to higher relaxation times. In addition, the LCB-2.5 displays a longer relaxation time than the L-PPs, illustrating that long-chain branches alter the stress relaxation mechanisms. Long-chain branches with slower motions such as arm retraction restrict the simple reptation that is expected for linear polymers.

Rheological characterization of the blends

The complex viscosities as a function of frequency for the L-25/LCB-2.5 and L-3.2/LCB-2.5 blends are plotted in Fig. 4a, b, respectively. These two blends are extreme cases and the other blends are intermediated. As seen in Fig. 4a, the complex viscosity of the L-25/LCB-2.5 blends at low frequencies is very small, a behavior which is the consequence of short molecular length of the L-25 that restricts the presence of entanglements. The complex viscosities of the blends at low frequencies increase dramatically with increasing the branched content. For the L-3.2/LCB-2.5 blends, with increasing the LCB-2.5 content shear-thinning is more pronounced.

To investigate the miscibility of the blends, a logarithmic mixing rule has been applied to the blends. The logarithmic mixing rule is represented as [29]

$$\log \eta_0(\omega) = \phi_\beta \log(\eta_0(\omega))_1 + (1 - \phi_\beta) \log(\eta_0(\omega))_2, \tag{3}$$

where ϕ_β and η_0 are the weight fraction of branched component and the zero-shear viscosity, respectively. For the L-25/LCB2.5 blends, as plotted in Fig. 5a, a good agreement with the logarithmic mixing rule is observed, suggesting that these blends are miscible. However, for the L-3.2 a deviation from the logarithmic mixing rule is observed for the branched contents higher than 50 wt% of the blends. This behavior has been reported for blends of linear and branched polypropylenes and polyethylenes in the literature [23]. It is believed that the molecular weights of the components as well as the amount of LCB content and the branching structure (e.g., tree-like or star-like) of the LCB component, influence the miscibility of the blends. Stange et al. [9] have demonstrated that the branching structure of the LCB-2.5 is tree-like and, as a consequence, represents a negative deviation from logarithmic mixing rule.

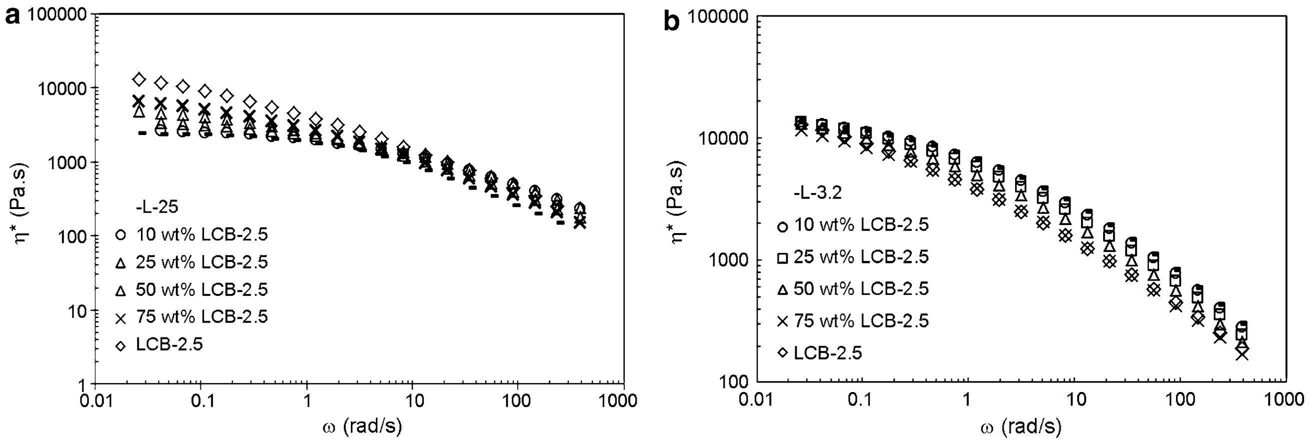

Fig. 4 Complex viscosity as a function of frequency for: **a** L-25/LCB-2.5, **b** L3.2/LCB-2.5 blends at $T = 180$ °C

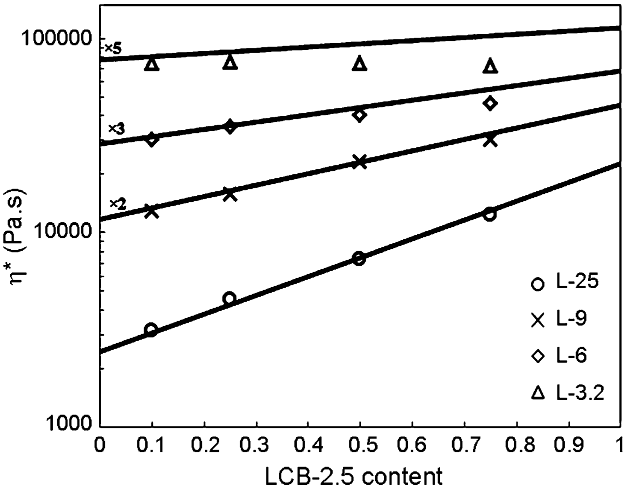

Fig. 5 Zero-shear viscosity as a function of LCB-2.5 content at $T = 180$ °C (*lines* represent the mixing rule)

For further investigation on the miscibility of the blends, the Cole–Cole plots ($\eta'' - \eta'$) of the blends are illustrated in Fig. 6. The radius of semi-circular shape is increased with increasing the molecular weight. For the L-25/LCB-25 blends the plots are intermediate, suggesting the miscibility of the blends. However, some synergistic effects for the L-3.2/LCB2.5 blends are obtained and no trend for the blends is observed. It is clear that with increasing molecular weight, the miscibility of the blends of L-PP and LCB-PP is reduced.

To investigate the effect of molecular weight of linear component on the relaxation behavior of the blends, the weighted relaxation spectra of the L-25/LCB2.5 and L-3.2/LCB-2.5 are shown in Fig. 7. It is clear that the addition of long-chain branched component alters the relaxation mechanism from the simple reptation, as expected for linear polymers, to the arm retraction, which postpones the movements of chains along their backbone; as a consequence the

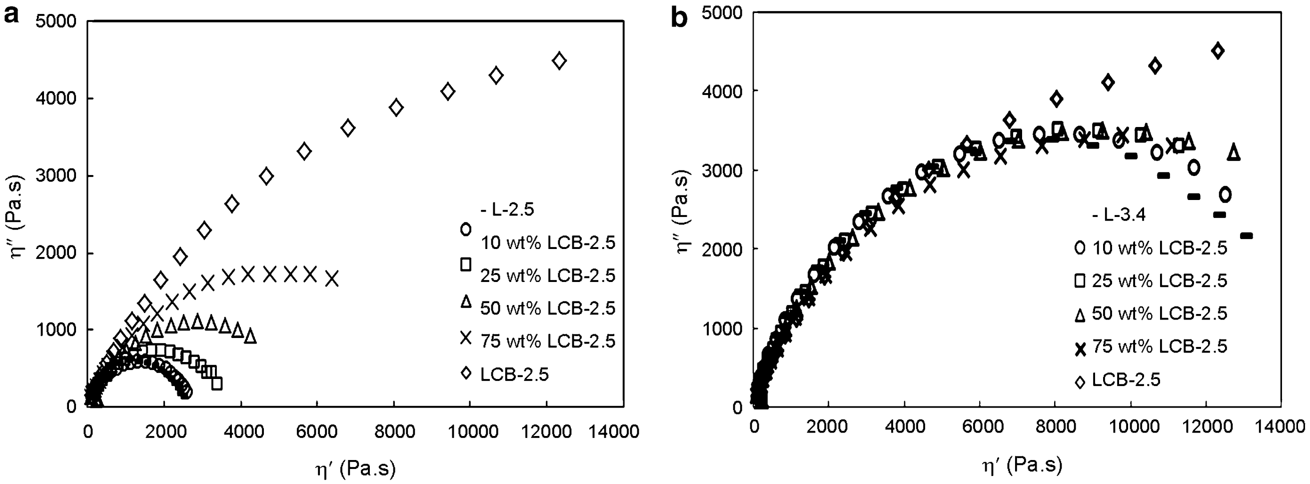

Fig. 6 Cole–Cole plots for: **a** L-25/LCB-2.5, **b** L-3.2/LCB2.5 blends at $T = 180$ °C

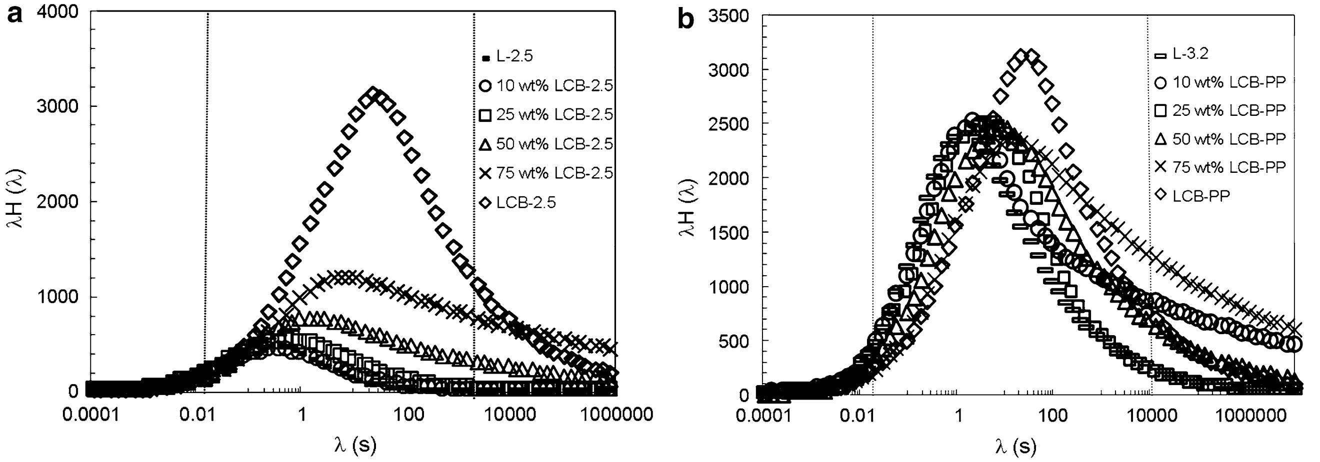

Fig. 7 Weighted relaxation spectra for: **a** L-25/LCB-2.5, **b** L-3.2/LCB2.5 blends at $T = 180$ °C

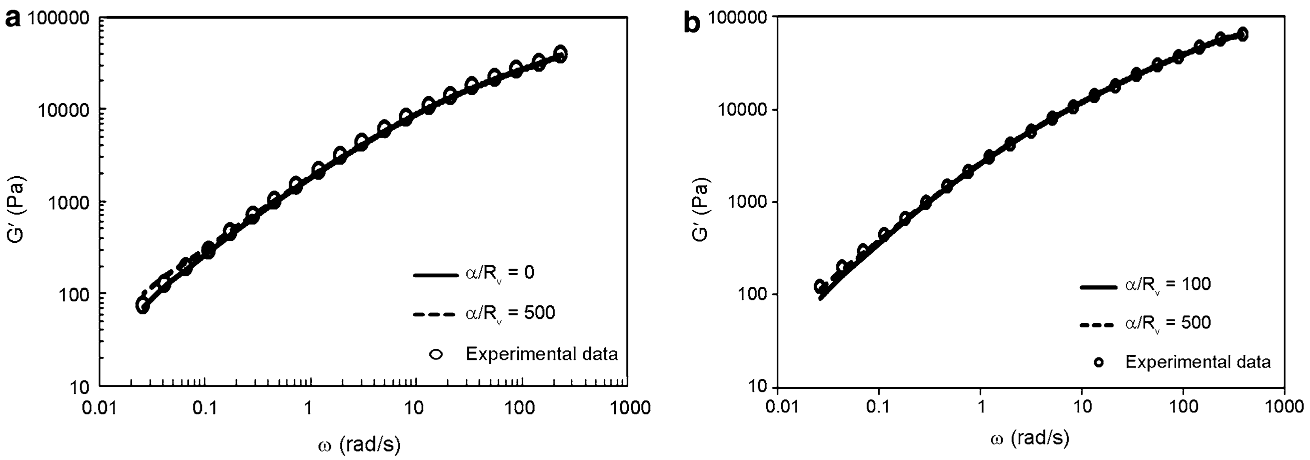

Fig. 8 Comparison between experimental data and prediction of storage modulus using Palierne model for: **a** (25/75) L-25/LCB2.5 blend, **b** (25/75) L-3.2/LCB2.5 blend at $T = 180$ °C

maxima in the curves shift to longer times and the spectrum shape becomes broader. As seen in Fig. 7a, for the L-25/LCB2.5, the peaks are intermediate to the neat polypropylenes, representing again miscibility; however, for the L-3.2/LCB-2.5 blends no specific trend is observed.

Only a few models have been developed to predict the linear viscoelastic behavior of polymer blends to correlate the viscoelastic properties of emulsion systems to microstructure. Furthermore, these models can correlate the dynamic response of polymer blends to the interfacial tension between their components and the morphology composition.

A model for predicting the linear viscoelastic properties of some immiscible emulsion-type blends has been developed by Palierne [30]. For a narrow distribution of incompressible droplet diameters as well as constant interfacial tension, the complex modulus of a blend is expressed by

$$G_{\mathrm{B}}^{*}(\omega) = G_{\mathrm{m}}^{*}(\omega)\frac{1 + 3\phi H^{*}(\omega)}{1 - 2\phi H^{*}(\omega)} \tag{4}$$

H^{*} is defined as

$$H^{*} = \frac{\left(\frac{\alpha}{R_v}\right)(2G_{\mathrm{m}}^{*}(\omega) + 5G_{\mathrm{d}}^{*}(\omega)) + (G_{\mathrm{d}}^{*}(\omega) - G_{\mathrm{m}}^{*}(\omega))(16G_{\mathrm{m}}^{*}(\omega) + 19G_{\mathrm{d}}^{*}(\omega))}{10\left(\frac{\alpha}{R_v}\right)(G_{\mathrm{d}}^{*}(\omega) + G_{\mathrm{m}}^{*}(\omega)) + (3G_{\mathrm{m}}^{*}(\omega) + 2G_{\mathrm{d}}^{*}(\omega))(16G_{\mathrm{m}}^{*}(\omega) + 19G_{\mathrm{d}}^{*}(\omega))} \tag{5}$$

α is the interfacial tension, ϕ is the volume fraction of the droplets with volume average radius of R_v, G_{d}^{*} and G_{m}^{*} are the complex moduli of the droplets and matrix, respectively. The storage and loss moduli of blends can be easily calculated using some simple algebraic equations [31]. These models, which have been modified for melt blends, show a good agreement with experimental data [32].

Measuring the dimension of droplets in the L-PPs and LCB-PP blends is impossible due to the low optical contrast between the PP components. Tabatabaei et al. [25] suggested α/R_v as a single parameter to find the best fits of experimental data for the blends. Here the influence of α/R_v (0 and 500) on the storage modulus for the blends of the L-25 and L-3.2 with 75 wt% LCB-2.5 is predicted by the Palierne model which the results are shown in Fig. 8a, b, respectively. For the blends of the other linear components (L-6 and L-9) with 75 wt% of LCB-2.5, the same trend as L-25 is obtained. In comparison, the predicted G' values at low frequencies are influenced by the values of α/R_v. As shown in Fig. 8a, for the (25/75) L-25/LCB2.5 blend the value of $\alpha/R_v = 0$ achieves a better fit of the model to the experimental data; however, for the (75/25) L-3.2/LCB2.5 blend, the value of $\alpha/R_v = 500$ is closer to the experimental data. The zero value of interfacial tension is an indication of miscibility, while other rheological investigation suggests the miscibility of the L-25/LCB2.5 blends. However, the non-zero value of interfacial tension seems to be a demonstration of the presence of a dispersed phase.

It should be noted that in immiscible blends the storage modulus at low frequencies increases while the loss modulus does not differ significantly [25]. The values of G'' predicted by the model are not sensitive to the values of α/R_v and are in good agreement with the experimental data.

Extensional data are very sensitive to the molecular structure. Several viscoelastic models can describe the

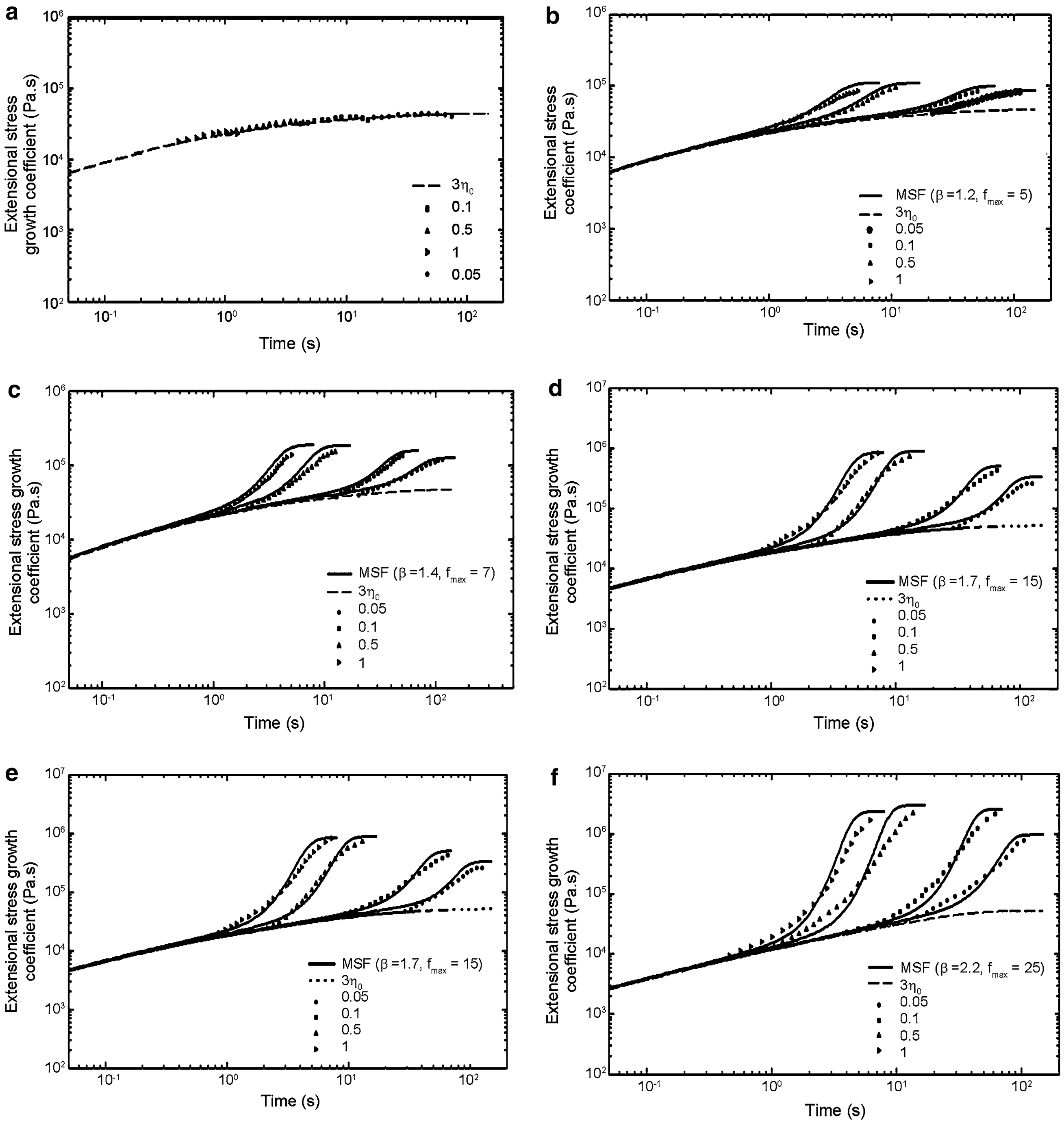

Fig. 9 Stress growth coefficients data in extension and prediction of MSF model for: **a** L-3.2, **b** 10 wt% LCB-2.5, **c** 25 wt% LCB-2.5, **d** 50 wt% LCB-2.5, **e** 75 wt% LCB-2.5, **f** LCB-2.5 at 180 °C

growth of stress during the uniaxial elongation of polymeric melts. By generalizing the Doi–Edwards model to the Molecular Stress Function (MSF) a successful prediction of the rheological behavior of linear and long-chain branched polymer melts in transient uniaxial constant extension-rate experiments is possible [33–35]. In the MSF model, the relative tension of the macromolecular chain in a tube segment of diameter, a, at time, t, is expressed by a Molecular Stress Function:

$$f(t,t') = a_0/a(t,t') \tag{6}$$

t' represents the time when the tube was created with equilibrium tube diameter a_0. The extra stress tensor is given by

$$\sigma(t) = \int_{-\infty}^{t} m(t-t')f^2(t,t')S_{\mathrm{DE}}^{\mathrm{IA}}(t,t')\mathrm{d}t', \tag{7}$$

where

$$m(t-t') = \frac{\partial G(t-t')}{\partial t'} = \sum_{i=1}^{N} \frac{g_i}{\lambda_i} e^{-\frac{t-t'}{\lambda_i}} \tag{8}$$

is the Maxwell memory function. According to the MSF model, the tension in a chain segment is related to the deformation history of the tube segments. $S_{\mathrm{DE}}^{\mathrm{IA}}$ indicates the strain measure of the Doi-Edwards model, using the independent alignment (IA) assumption:

$$S_{\mathrm{DE}}^{\mathrm{IA}} = 5f^2\left\langle \frac{\mathrm{u}'\mathrm{u}'}{u'^2} \right\rangle = 5S_{\mathrm{DE}}, \tag{9}$$

where S_{DE} is the second-order orientation tensor and $\langle \cdots \rangle$ denotes an average over an isotropic distribution function of unit vectors, and u' is the length of the unit vector $\mathbf{u}'$.

In elongational deformations the evolution equation is expressed by

$$\frac{\partial f^2}{\partial t} = \dot{\varepsilon}\, \frac{\beta f^2}{1+\frac{\beta-1}{f^4}} \left(S_{11} - S_{33} - \frac{f(f^3-1)}{f_{\max}(f_{\max}^3-1)} \sqrt{S_{11} + \frac{1}{2}S_{33}} \right) z \tag{10}$$

S_{11} and S_{33} are the respective components of the orientation tensor parallel and perpendicular to the direction of elongation. It should be noted that the parameter β describes the topology of the melt and indicates the slope of the transient elongational viscosity curve. When the tube is stretched, one segment is extended, while $(\beta - 1)$ segments are compressed.

The time-dependent elongational viscosities ($\eta_E^{+}(t, \dot{\varepsilon}_0)$) of the L3.2/LCB2.5 blends are presented in Fig. 9a–f and compared to the prediction of the MSF model. For the linear polypropylene, all the curves measured at different strain rates have superimposed on the linear viscoelastic curve. The transient elongational viscosity is calculated by

$$\eta_{\mathrm{E}}^{+} = 3\eta^{+} = 3\sum_{i} \frac{g_i}{\lambda_i}\left[1 - \exp\left(-\frac{t}{\lambda_i}\right)\right], \tag{11}$$

where g_i and λ_i are the discrete relaxation spectra calculated from the Maxwell model and are shown for the L-3.2 blends in Table 2.

A significant strain hardening takes place upon addition of low amounts of the LCB-PP. Deviations from the linear viscoelasticity at shorter times and sharper increase in the elongational viscosity were found as the weight fraction of the LCB-PP increase.

A good agreement between the elongational viscosities and MSF model is observed. The range of values of the β

Table 2 Relaxation spectra of L-3.2 blends at $T = 180$ °C

L-3.2		10 wt% LCB-2.5		25 wt% LCB-2.5		50 wt% LCB-2.5		75 wt% LCB-2.5		LCB-2.5	
g_i (Pa)	λ_i (s)	g_i (Pa)	λ_i (s)	g_i (Pa)	λ_i (s)	g_i (Pa)	λ_i (s)	g_i (Pa)	λ_i (s)	g_i (Pa)	λ_i (s)
9.31×10^4	1.08×10^{-3}	1.10×10^5	7.94×10^{-4}	1.61×10^5	6.61×10^{-4}	2.08×10^5	3.55×10^{-5}	7.35×10^4	5.59×10^{-4}	1.33×10^5	5.87×10^{-4}
3.61×10^4	1.46×10^{-2}	3.63×10^4	1.17×10^{-3}	3.36×10^4	1.03×10^{-3}	5.54×10^4	6.81×10^{-4}	2.74×10^4	2.30×10^{-3}	9.19×10^4	1.31×10^{-4}
2.84×10^4	3.97×10^{-2}	2.67×10^4	3.05×10^{-3}	1.90×10^4	4.04×10^{-2}	3.39×10^4	9.69×10^{-3}	2.04×10^4	9.48×10^{-3}	1.57×10^4	1.18×10^{-2}
1.98×10^4	5.36×10^{-2}	2.09×10^4	4.48×10^{-2}	1.05×10^4	1.59×10^{-2}	1.69×10^4	5.06×10^{-3}	1.17×10^4	3.90×10^{-2}	9.46×10^4	2.63×10^{-3}
1.11×10^4	1.97×10^{-1}	1.16×10^4	1.72×10^{-1}	8.70×10^3	2.60×10^{-1}	1.44×10^4	1.86×10^{-3}	6.26×10^3	1.61×10^{-1}	7.49×10^3	5.30×10^{-2}
3.96×10^3	7.25×10^{-1}	4.19×10^3	6.60×10^{-1}	4.24×10^3	6.26×10^{-1}	8.22×10^3	2.64×10^{-1}	2.85×10^3	6.61×10^{-1}	3.76×10^3	2.38×10^{-1}
1.29×10^3	2.67×10^0	1.41×10^3	2.53×10^0	1.40×10^3	2.46×10^0	2.15×10^3	1.38×10^0	1.06×10^3	2.72×10^0	1.87×10^3	1.07×10^0
2.09×10^2	9.80×10^0	2.47×10^2	9.71×10^0	3.10×10^2	9.7×10^0	9.08×10^2	7.20×10^0	2.70×10^2	1.12×10^1	6.03×10^2	4.78×10^0
7.42×10^1	3.60×10^1	9.04×10^1	3.73×10^1	9.58×10^1	3.82×10^1	1.05×10^2	3.76×10^1	9.94×10^1	4.61×10^1	5.17×10^2	2.15×10^1

parameter in this work varies from 1 for the L-3.2 to 2.2 for the LCB-2.5 which are in accordance with 1 for the linear polymer and 2 for the long-chain branched polymer, respectively [36]. Furthermore, $f^2_{\max}$ which represents the maximum amount of energy stored in a tube segment, increases with amount of LCB-2.5 in the blends.

Conclusions

In this study, the shear and extensional rheological properties of the blends of L-PPs having different molecular weights and LCB-PP were investigated. Based on the log-additivity rule, for the zero-shear viscosity, weighted relaxation spectra, Cole–Cole plots and Palierne model, the blends of low molecular weight linear polypropylene showed miscibility while for high molecular weight L-PPs and higher amount of LCB-PP, immiscibility was observed. The Palierne model predictions were in good agreement with the experimental data.

With adding a small amount of LCB-PP, significant strain hardening was observed. The Molecular Stress Function could predict the strain hardening behavior of the blends.

Acknowledgments We gratefully acknowledge Dr. SH. Tabatabaei for his valuable ideas throughout this paper.

References

1. Palza H, Quijada R, Wilhelm M (2013) Effect of short-chain branching on the melt behavior of polypropylene under small-amplitude oscillatory shear conditions. Macromol Chem Phys 214:107–116
2. Gotsis AD, Zeevenhoven BLF, Tsenoglou C (2004) Effect of long branches on the rheology of polypropylene. J Rheol 48:895–914
3. Zulli F, Andreozzi L, Passaglia E, Augier S, Giordano M (2013) Rheology of long-chain branched polypropylene copolymers. J Appl Polym Sci 127:1423–1432
4. Nam GJ, Yoo JH, Lee JW (2005) Effect of long-chain branches of polypropylene on rheological properties and foam-extrusion performances. J Appl Polym Sci 96:1793–1800
5. Gotsis AD, Zeevenhoven BLF, Hogt AH (2004) The effect of long chain branching on the processability of polypropylene in thermoforming. Polym Eng Sci 44:973–982
6. Bailly M, Kontopoulou M (2009) Preparation and characterization of thermoplastic olefin/nanosilica composites using a silane-grafted polypropylene matrix. Polymer 50:2472–2480
7. Lee GW, Jagannathan S, Chae HG, Minus ML, Kumar S (2008) Carbon nanotube dispersion and exfoliation in polypropylene and structure and properties of the resulting composites. Polymer 49:1831–1840
8. Almeida LA, Marques MFV, Dahmouche K (2015) Synthesis of polypropylene/organoclay nanocomposites via in situ polymerization with improved thermal and dynamic-mechanical properties. J Nanosci Nanotechnol 15:2514–2522
9. Stange J, Uhl C, Münstedt H (2005) Rheological behavior of blends from a linear and a long-chain branched polypropylene. J Rheol 49:1059–1079
10. Li S, Xiao M, Wei D, Xiao H, Hu F, Zheng A (2009) The melt grafting preparation and rheological characterization of long chain branching polypropylene. Polymer 50:6121–6128
11. Borsig E, van Duin M, Gotsis AD, Picchioni F (2008) Long chain branching on linear polypropylene by solid state reactions. Eur Polym J 44:200–212
12. Krause B, Stephan M, Volkland S, Voigt D, Häußler L, Dorschner H (2006) Long-chain branching of polypropylene by electron-beam irradiation in the molten state. J Appl Polym Sci 99:260–265
13. Lugão AB, Otaguro H, Parra DF, Yoshiga A, Lima LFCP, Artel BWH, Liberman S (2007) Review on the production process and uses of controlled rheology polypropylene-gamma radiation versus electron beam processing. Radiat Phys Chem 76:1688–1690
14. Graebling D (2002) Synthesis of branched polypropylene by a reactive extrusion process. Macromolecules 35:4602–4610
15. Mogilicharla A, Majumdar S, Mitra K (2015) Multiobjective optimization of long-chain branched propylene polymerization. Polym Eng Sci 55:1067–1076
16. Auhl D, Stange J (2004) Long chain branched polypropylenes by electron beam irradiation and their rheological properties. Macromolecules 37:9465–9472
17. Guapacha J, Failla MD, Vallés EM, Quinzani LM (2014) Molecular, rheological, and thermal study of long-chain branched polypropylene obtained by esterification of anhydride grafted polypropylene. J Appl Polym Sci 131:40357–40369
18. Ahirwal D, Filipe S, Neuhaus I, Busch M, Schlatter G, Wilhelm M (2014) Large amplitude oscillatory shear and uniaxial extensional rheology of blends from linear and long-chain branched polyethylene and polypropylene. J Rheol 58:635–658
19. Hyun K, Ahn KH, Lee SJ, Sugimoto M, Koyama K (2006) Degree of branching of polypropylene measured from Fourier-transform rheology. Rheol Acta 46:123–129
20. Chikhalikar K, Banik S, Azad LB, Jadhav K, Mahajan S, Ahmad Z, Kulkarni S, Gupta S, Doshi P, Pol H, Lele A (2014) Extrusion film casting of long chain branched polypropylene. Polym Eng Sci. doi:10.1002/pen.24039
21. Spitael P, Macosko CW (2004) Strain hardening in polypropylenes and its role in extrusion foaming. Polym Eng Sci 44:2090–2100
22. McCallum TJ, Kontopoulou M, Park CB, Muliawan EB, Hatzikiriakos SG (2007) The rheological and physical properties of linear and branched polypropylene blends. Polym Eng Sci 47:1133–1140
23. Fang Y, Sadeghi F, Fleuret G, Carreau PJ (2008) Properties of blends of linear and branched polypropylenes in film blowing. Can J Chem Eng 86:6–14
24. Wagner MH, Kheirandish S, Stange J, Münstedt H (2006) Modeling elongational viscosity of blends of linear and long chain branched polypropylenes. Rheol Acta 46:211–221
25. Tabatabaei SH, Carreau PJ, Ajji A (2009) Rheological and thermal properties of blends of a long-chain branched polypropylene and different linear polypropylenes. Chem Eng Sci 64:4719–4731
26. Wang L, Wan D, Zhang Z, Liu F, Xing H, Wang Y, Tang T (2011) Synthesis and structure–property relationships of polypropylene-*g*-poly(ethylene-*co*-1-butene) graft copolymers with well-defined long chain branched molecular structures. Macromolecule 44:4167–4179
27. Wood-Adams PM, Dealy JM, deGroot AW, Redwine OD (2000) Effect of molecular structure on the linear viscoelastic behavior of polyethylene. Macromolecules 33:7489–7499
28. Honerkamp J, Weese J (1993) A nonlinear regularization method for the calculation of relaxation spectra. Rheol Acta 32:65–73
29. Utracki LA, Schlund B (1987) Linear low density polyethylenes and their blends: part 4 shear flow of LLDPE blends with LLDPE and LDPE. Polym Eng Sci 27:1512–1522

30. Palierne JF (1990) Linear rheology of viscoelastic emulsions with interfacial tension. Rheol Acta 29:204–214
31. Hussein IA, Williams MC (2001) Rheological study of the miscibility of LLDPE/LDPE blends and the influence of T_{mix}. Polym Eng Sci 41:696–701
32. Ajili SH, Ebrahimi NG, Ansari M (2008) Rheological study of segmented polyurethane and polycaprolactone blends. Rheol Acta 47:81–87
33. Wagner MH, Rubio P, Bastian H (2001) The molecular stress function model for polydisperse polymer melts with dissipative convective constraint release. J Rheol 45:1387–1412
34. Abbasi M, Golshan Ebrahimi N, Nadali M, Khabazian Esfahani M (2012) Elongational viscosity of LDPE with various structures: employing a new evolution equation in MSF theory. Rheol Acta 51:163–177
35. Rolón-Garrido VH (2014) The molecular stress function (MSF) model in rheology. J Rheol 53:663–700
36. Wagner MH, Yamaguchi M, Takahashi M (2003) Quantitative assessment of strain hardening of low-density polyethylene melts by the molecular stress function model. J Rheol 47:779–793